Published in "Journal of Organometallic Chemistry 692(26): 5709-5716 , 2007"
which should be cited to refer to this work.

Theoretical investigation of the bonding properties of *N*-heterocyclic carbenes coordinated to electron-rich d^8 metal centers

Emmanuel F. Penka [a], Carl W. Schläpfer [a], Michael Atanasov [a,b], Martin Albrecht [a,*], Claude Daul [a,*]

[a] *Department of Chemistry, University of Fribourg, Chemin du Musee 9, CH-1700 Fribourg, Switzerland*
[b] *Institute of General and Inorganic Chemistry, Bulgarian Academy of Sciences, 1113 Sofia, Bulgaria*

http://doc.rero.ch

Abstract

Density functional theory (DFT) at the generalized gradient approximation (GGA) level has been applied for the analysis of the bond between group 10 metals and *N*-heterocyclic carbene (NHC) in complexes $[MX_3(NHC)]^-$ (M = Ni, Pd, Pt, X = H, Cl, I). For comparative purposes, similar calculations have been performed for analogous pyridine complexes $[MX_3(py)]^-$ (py = pyridine). Full geometry optimizations have been performed for all complexes. The role of the M–L π interaction was investigated by the aid of respectively, energy decomposition analysis, Hirshfeld atomic charge variation, molecular orbital considerations and bond order decomposition analysis. The π-bonding contribution increases in the order I < Cl < H, and Pt < Pd < Ni. Most significantly, the absolute π-acceptor ability of the NHC in these complexes is larger than that of pyridine. However, due to the dominant σ donor interactions, the relative contribution, that is the π/σ ratio, is predicted to be smaller.

Keywords: *N*-heterocyclic carbene bonding; Group 10 metals; π-Interactions; Energy decomposition analysis; Hirshfeld atomic charge

1. Introduction

Ligand tuning is one of the most powerful concepts for tailoring the (catalytic) properties of transition metal centers. It is therefore particularly relevant to understand the nature of the metal–ligand bonding. Classical donor ligands such as amines, imines, phosphines, phosphites, or sulfides, have been studied extensively and their bonding properties are well-established and provide a very useful toolbox for organometallic chemistry [1].

Less evident are the donor properties of imidazolium-derived *N*-heterocyclic carbenes (NHCs), an increasingly important class of ligands [2]. Although NHCs were successfully used as ligands already some 40 years ago through the pioneering work of Wanzlick, Oefele, Stone, and Lappert [3], their popularity only increased with Arduengo's discovery that appropriately modified NHCs can be isolated and characterized, and that they are air- and moisture-stable [4]. Since then, a large number of transition metal complexes comprising NHC ligands have been prepared. Many of them provided highly active catalysts for a variety of transformations, with Grubbs' 2nd generation olefin metathesis catalyst as the presumably most prominent example [5].

Initially, NHCs have been supposed to be pure σ donor ligands [6]. Based on qualitative orbital considerations, the π acceptor properties have been postulated to be negligible, since the formally empty carbon p-orbital was assumed to be stabilized by π donation from the adjacent nitrogens rather than from (filled) metal d orbitals. Recently however, this assumption has been challenged by a number of experimental [7] and computational studies [8]. A

* Corresponding authors. Fax: +41 26 3009738.
E-mail addresses: martin.albrecht@unifr.ch (M. Albrecht), claude.daul@unifr.ch (C. Daul).

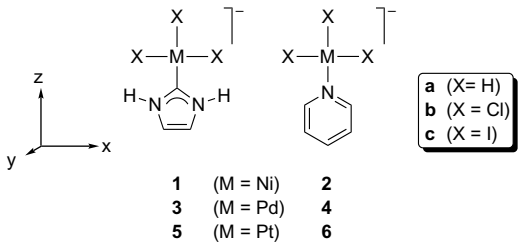

Fig. 1. Complexes analyzed in this work, including the adopted complex numbering and axis labeling scheme.

consensus of these studies appears to be that M → NHC π backbonding interactions may become significant with electron-rich metal centers. For example we have shown that the donor–acceptor properties of NHC and pyridine are virtually identical when coordinated to a Fe(cp) fragment [7g]. Taking into account the high σ donor power of NHC and the well-known π acceptor properties of pyridine, also significant π acceptor properties of NHC ligands need to be postulated in order to explain the observed electronic similarity of NHC and pyridine.

Here, we have expanded the theoretical understanding of NHC bonding to electron-rich transition metals. For this purpose, the structural and electronic properties of a series of square-planar anionic d^8 complexes of type $[MX_3L]^-$ (M = Ni, Pd, Pt and L = NHC, pyridine, Fig. 1) have been analyzed. The influence of the metal-bound anion X on the M–L bond has been identified by gradually increasing M–X π interactions. Hence, X has been modulated from purely σ donating (X = H) to weakly π bonding (X = Cl) to relatively strongly π bonding (X = I). Calculations on the corresponding bromide complexes (X = Br) did not reveal particular features. The results are therefore provided in the supplementary information. The specific M–L σ and π bond interactions are discussed based on the results of a variety of methods including energy decomposition, atomic charge variation, and bond order analysis [9]. Our results consistently indicate π acceptor abilities of the NHC ligand that are, on an absolute scale, larger than for pyridine. These findings are in good agreement with previously reported experimental work.

2. Computational details

The DFT calculations were performed using the ADF2006.01 package [10,11]. The local density approximation (LDA) characterized by the Vosko–Willk–Nusair (VWN) parametrization has been adopted for the geometry optimization [12]. PW91 generalized gradient approximation (GGA) exchange-correlation functional have been used for energy calculation [13]. Large Slater-type orbital (STO) basis sets (triple-ζ) without frozen core approximation were employed as basis functions to describe the atomic orbitals on each atom. The relativistic extension of LCAO program using the zero-order regular approximation (ZORA) by Snijders et al. has been applied to take into account the relativistic effect on the metal [14]. The geometry optimization has been performed under C_{2v} symmetry. Integrals were numerically calculated with an accuracy of ten digits. In addition, frequency calculations were performed to check if the stationary points were potential minima.

The bonding interactions in $[MX_3L]^-$ have been analyzed by means of orbital interactions [15], Hirshfeld charge analysis [16], bond order decomposition [17], and Morokuma-type energy decomposition analysis (EDA) [18] developed by Ziegler and Rauk for DFT methods and incorporated in ADF [19]. The atomic orbital population has been analyzed with the aid of natural orbitals [20]. Natural population analysis (NPA) is an alternative method to the conventional Mulliken population analysis [21] and seems to exhibit improved numerical stability and gives a better description of the electron distribution in compounds of highly ionic character [20,22].

All complexes have been analyzed by using molecular orbital diagrams to study the electronic interaction between the two molecular fragments $[MX_3]^-$ and the ligand L. DFT energies of the charged $[MX_3]^-$ fragment and the neutral ligand have been referenced to the energy of a set of low-lying ligand-centered $1s^2$ (C) and $1s^2$ (N) orbitals in order to compensate electrostatic effects. As a consequence, the ligand MO energies of the free NHC and pyridine ligand have been increased [23]. Natural atomic orbital populations have been calculated with the aid of the general stand-alone GENNBO version of NBO 5.O program [24]. Bond order decomposition analysis and density deformation analysis have been made using in-house developed Mathlab programs, which have been interfaced with the ADF program package [25].

3. Results and discussions

3.1. Geometry

The relevant structural parameters of the $[PdX_3L]^-$ complexes as predicted by our calculations are summarized in Table 1. Since no experimental data of these complexes have been reported thus far, we have compared our results with related crystallographically characterized complexes **7** and **8** (Fig. 2) [26,27]. The pertinent bond lengths and angles are generally in good agreement with the computed values.

The calculated Pd–L bond length and the L–Pd–X angle are generally larger for the pyridine complexes than for their NHC homologs. As expected, the Pd–X_{trans} bonds are longer for complexes with NHC than with pyridine, reflecting the higher *trans* influence. According to the calculated values, the *trans* influence decreases from H > NHC > Cl > py. The large Pd–I_{trans} distance calculated for the iodide complexes may be attributed to the large size of the three coordinating iodide nuclei rather than to a direct *trans* influence. Such steric arguments are further supported by the relatively long Pd–L bond dis-

http://doc.rero.ch

Table 1
Selected structural parameters of the optimized structures $[PdX_3L]^-$ **3** and **4** [a]

$[PdX_3L]^-$	Parameter	L = NHC (**3**)		L = pyridine (**4**)	
		Calc	Exp [26a]	Calc	Exp [27a]
$[PdH_3L]^-$ (**a**)	$Pd–H_{cis}$	1.66		1.66	
	$Pd–H_{trans}$	1.61		1.56	
	Pd–L	1.96		2.06	
	H–Pd–L	91.3		95.0	
$[PdCl_3L]^-$ (**b**)	$Pd–Cl_{cis}$	2.30	2.35	2.31	2.37
	$Pd–Cl_{trans}$	2.32		2.26	2.33
	Pd–L	1.93		2.04	2.05
	Cl–Pd–L	86.6		91.8	87.1
$[PdI_3L]^-$ (**c**)	$Pd–I_{cis}$	2.64	2.62	2.64	
	$Pd–I_{trans}$	2.64	2.69	2.59	
	Pd–L	1.97	1.99	2.11	
	I–Pd–L	89.5	86.7	93.4	

[a] Bond lengths in Å, angles in °.

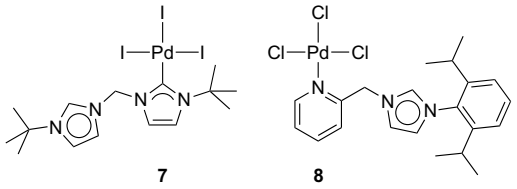

Fig. 2. Transition metal complexes used for structural comparison.

tance, which corroborates the experimental data. Furthermore, the optimized L–Pd–X angle in all complexes is close to 90° with the highest value observed for **4a** (py-Pd–H = 95.0°) and the lowest for **3b** (NHC–Pd–Cl = 86.6°).

The stability of the complexes has been investigated by calculating the total energy as a function of the dihedral angle θ between the ligand L and the planar fragment $[PdCl_3]^-$ (Fig. 3). The NHC-containing complex **3a** shows

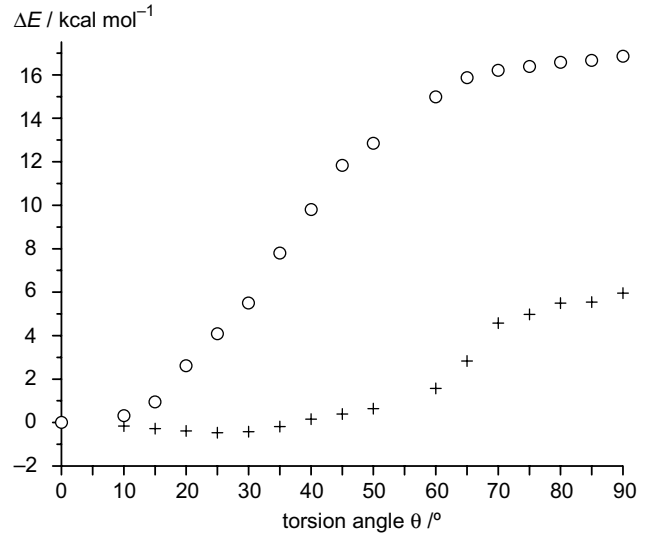

Fig. 3. Variation of the total energy of the NHC complex **3a** (o) and the pyridine complex **4a** (+) as a function of the dihedral angle θ between $[PdCl_3]^-$ and the ligand L.

an energy minimum in a planar conformation ($\theta = 0°$). The pyridine analog **4a** reveals a shallow minimum around $\theta = 25°$ with an energy difference of less than 1 kcal mol^{-1}. This may reflect a fluxional behavior of the pyridine ring comprising a wiggeling of the pyridine about the Pd–N axis. With both ligands, an orthogonal orientation is the least favored conformation. Notably, the energy barrier for free rotation about the Pd–L bond is significantly larger for NHC than for pyridine.

3.2. Analysis of the electronic structure

Although π bonding arises from the sum of all interactions with π symmetry, it is reasonable to assume that the dominant contributions originate from frontier orbital interactions including the highest occupied and lowest unoccupied molecular orbitals (HOMO–LUMO). The HOMO–LUMO interactions have been calculated for **3** and **4** by combining the in-plane and out-of-plane orbitals of the fragment L with the matching orbitals of the $[PdX_3]^-$ fragment, that is $\pi(b_1)$ and $\pi(b_2)$, respectively. The $\pi(b_1)$ contribution appeared to be negligibly small as a consequence of the sp^2 hybridization of the metal-bound ligand atom, while out-of-plane interactions involving $\pi(b_2)$ are significant.

Fig. 4 shows the frontier orbital diagram including the symmetry-allowed interactions between the d–$\pi(b_2)$ orbitals of the $[PdX_3]^-$ fragment and the ligand orbitals. Representative interactions are depicted with their corresponding phase. The contribution of the $[PdX_3]^-$ fragment to the antibonding MO of $[PdX_3L]^-$, that is to the π^* M–L interaction, follows the trend H > Cl ≈ I. In complex **3**, these contributions amount to 10%, 5.3%, and 4.5%, respectively; in the pyridine complex **4**, they are slightly lower. The energy of the LUMO of the NHC ligand is significantly higher than the pyridine LUMO. As a consequence, the π interaction is larger in the complexes $[PdX_3(py)]^-$ **4** than in the analogous NHC complexes **3**. The energy of the HOMO $\pi(b_2)$ of $[MX_3]^-$ follows the order H > Cl > I. A stabilizing π back-bonding interaction is apparent between $[PdH_3]^-$ and the ligand LUMO, whereas with $[PdCl_3]^-$ and $[PdI_3]^-$, this interaction is destabilizing due to increased mixing in of the HOMO of the ligand.

As qualitatively detectable from the phase representation, the orbital overlap in the π bonding MO is very small for the hydride complexes $[PdH_3L]^-$ **3a** and **4a**. This overlap is considerably larger for the chloride and iodide complexes **3b** and **3c**, while for pyridine analogs **4b** and **4c**, only little overlap has been found. The π backbonding may be described in a first approximation of perturbation theory by considering the orbital overlap and the energy difference between the $[MX_3]^-$ HOMO and the LUMO of the ligand exclusively (HOMO–LUMO gap). Hence, energy differences have been determined from the equilibrium geometries of the corresponding complex $[MX_3(L)]^-$. Simultaneously, the corresponding d_{yz} orbital coefficient

http://doc.rero.ch

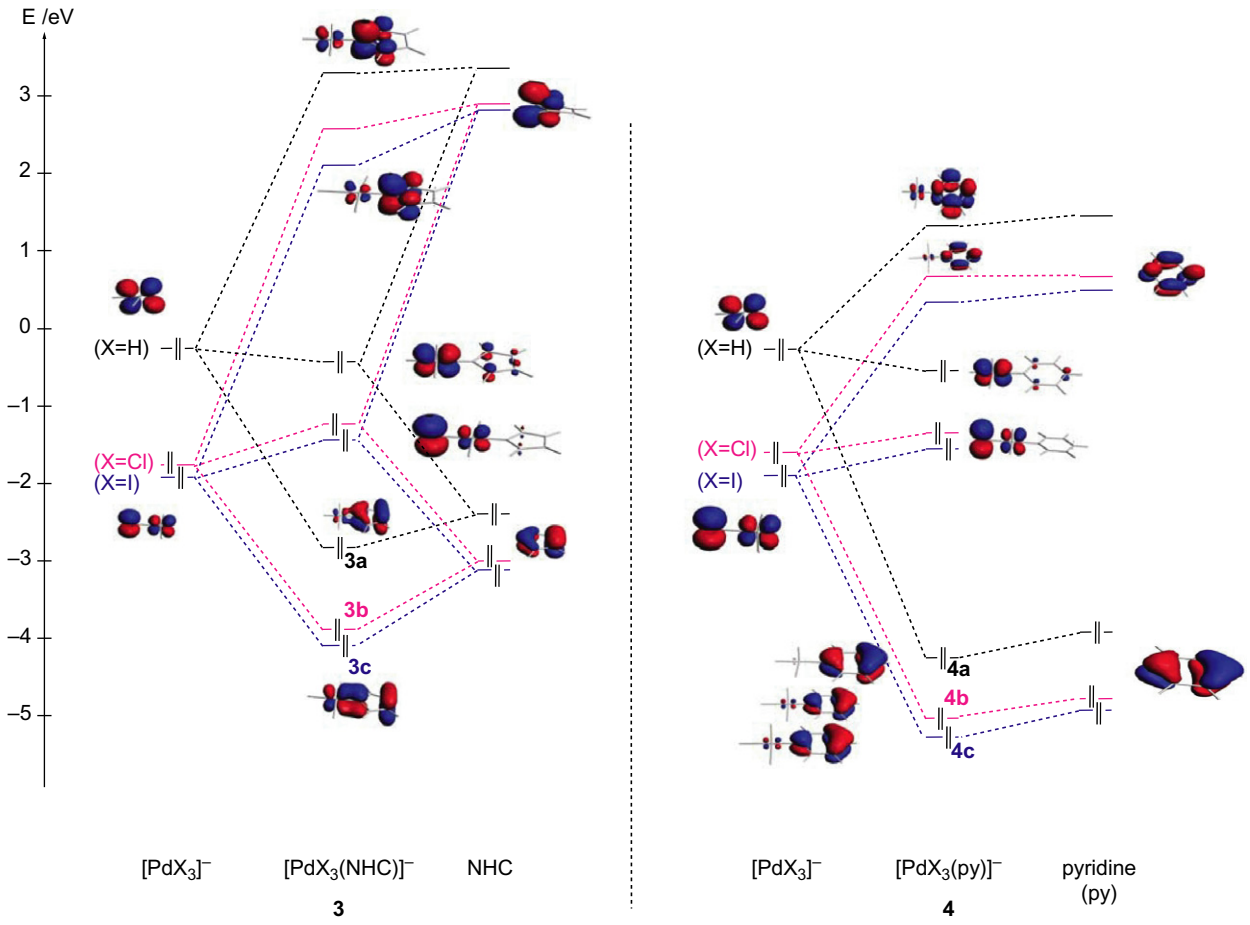

Fig. 4. Qualitative molecular orbital scheme for complexes **3** (left) and **4** (right) showing the out-of-plane $\pi(b_2)$ interactions. The MO energies of pyridine (py) and the NHC ligand are referenced to ligand-centered orbital energies in the corresponding complexes.

http://doc.rero.ch

of the HOMO has been used to estimate the overlap integral and hence the qualitative π backbonding interactions (Fig. 5). A number of general trends emerge from these calculations. The d_{yz} contribution is significantly larger for NHC than for py, and increases from I < Cl < H. This trend is particularly pronounced in Pt–NHC complexes. A reverse trend in terms of π bonding can be established from HOMO–LUMO energy gap analysis. The gap is consistently larger for NHC complexes by approximately 2 eV. Furthermore, the energy difference decreases when changing X from I < Cl ≪ H and from Pd ≈ Pt < Ni. These trends are in good agreement with the expected affinity of these fragments for covalent bonding. While orbital overlap and energy gap analysis show opposite and hence not conclusive trends when changing L from pyridine to NHC, they suggest that π backbonding is substantially more relevant in the hydride complexes than in the halides (Cl > I).

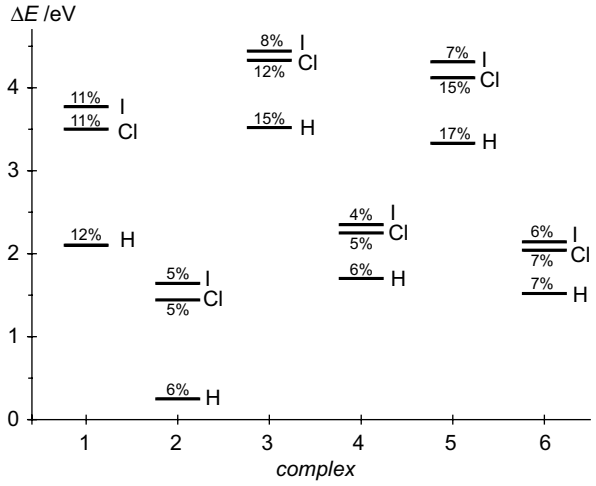

Fig. 5. HOMO–LUMO $\pi(b_2)$ orbital energy differences determined from Kohn–Sham MO energies of $[MX_3]^-$ fragments (HOMO) and the ligand LUMO in their equilibrium geometry conformation as determined in the complex $[MX_3(L)]^-$. The numbers indicate the overlap percentage.

3.3. Energy and charge decomposition analysis

Bonding analysis using the extended transition state method (ETS) has been recognized as a very useful approach for decomposing the bonding energy between the constituting components of a complex [28]. For complexes $[MX_3L]^-$, we have selected $[MX_3]^-$ and L as reference fragments in their appropriate geometry. This choice

http://doc.rero.ch

excludes M–X and X_{cis}–X_{trans} interactions and is focusing purely on the M–L bonding. Notably, the preparation of such fragments requires a large amount of energy ΔE_{Prep}, including the ionization energies for obtaining M^{2+} and X^-, and additional repulsive energy required to bring the X^- ions from infinity to their actual positions in the complex. Values for ΔE_{Prep} of the fragments have not been computed in this work since they do not contribute to the characterization of π interactions.

The results from the energy decomposition analysis are compiled in Table 2. The total bonding energy, ΔE, is expressed as the sum of Pauli repulsion, electrostatic and orbital energy (Eq. (1)):

$$\Delta E = \Delta E_{Pauli} + \Delta V_{Elst} + \Delta E_{Orb} \quad (1)$$

ΔE values are higher for complexes with NHC than with pyridine as expected for high covalent bonding for NHC ligands vs dative interactions in pyridine. For all complexes, the Pauli energy term is dominating and consequently, the sum $\Delta E_{Pauli} + \Delta V_{Elst}$ is positive. A higher repulsion is noted for complexes with NHC as compared with pyridine, probably because the most stable conformation for the pyridine complexes is twisted from planar. The ΔE_{Orb} term reflects the covalent character of the M–L bond; it is generally higher for the halide complexes than for the hydrides, and also higher for NHC than for pyridine complexes. In complexes with C_{2v} symmetry, the orbital energy ΔE_{Orb} is composed of the following components (Eq. (2)):

$$\Delta E_{Orb} = \Delta E_{Orb}(a_1) + \Delta E_{Orb}(a_2) + \Delta E_{Orb}(b_1) + \Delta E_{Orb}(b_2) \quad (2)$$

The $\Delta E_{Orb}(a_2)$ term is negligible and has not been considered further, but it can be easily deduced via Eq. (2). Apart from the nickel hydrides, the ΔE_{Orb} is dominated by the a_1 component, i.e. by the σ bond. Generally, the σ bonding of NHC is 50–100% stronger than of pyridine, which reflects the covalent character of the metal-carbene bond. Variation of the halide has little effect, while hydrides reduce the σ component of the H_3M–L bond. The $\Delta E_{Orb}(b_2)$ values are a direct probe for π interactions and are generally highest for metal hydrides. In the complex $[NiH_3(py)]^-$, **1a**, π bonding provides nearly 50% to the total orbital contribution of the Ni–pyridine bond. The absolute values of the π interactions in all (but the NiH_3) NHC complexes are higher than in the analogous pyridine species, indicating that π backbonding to the ligand is significant. Due to the strong metal-carbene σ bond, i.e. the large contribution from the a_1 term, the relative contribution of π interactions to the overall bond is generally slightly smaller than in pyridines. Only in a few cases (*e.g.* in the Pd and Pt halides featuring a soft metal center and not purely σ donating ligands X) the relative values are virtually equivalent. This suggest that π backbonding in NHC complexes may be relevant, in particular in combination with electron rich metal centers such as in metal-hydride fragments.

Our calculations reveal an unexpectedly large value of $\Delta E_{Orb}(b_1)$, for π in-plane interactions. MO and density deformation analysis of $[PdCl_3L]^-$ with coplanar and orthogonal orientation of L indicate that the b_1 value is best described by charge transfer of the halide in *cis* position of the $[PdCl_3]^-$ fragment to the antibonding orbital of the N–H and the C–H_{ortho} bond of the NHC and pyridine ligand, respectively [23]. Hence, these interactions do not contribute directly to the metal–carbene and metal–pyridine bond and will not be considered any further in the following discussion.

The pertinent metal–ligand bonding interaction and in particular the presence of π backbonding interactions has

Table 2
Energy decomposition analysis of $[MX_3L]^-$ from ionic $[MX_3]^-$ and neutral L[a]

	Complex	ΔE	ΔV_{Elst}	ΔE_{Pauli}	ΔE_{Orb}	$\Delta E_{Orb}(a_1)$	$\Delta E_{Orb}(b_1)$[b]	$\Delta E_{Orb}(b_2)$[b]
1a	$[NiH_3(NHC)]^-$	−2.10	−7.43	8.31	−2.95	−1.33	−0.49 (17)	−1.09 (37)
1b	$[NiCl_3(NHC)]^-$	−3.94	−8.93	10.36	−3.94	−2.72	−0.56 (14)	−0.63 (16)
1c	$[NiI_3(NHC)]^-$	−2.44	−8.38	9.74	−3.82	−2.61	−0.60 (16)	−0.56 (15)
2a	$[NiH_3(py)]^-$	−1.46	−4.87	5.80	−2.39	−0.86	−0.28 (12)	−1.16 (49)
2b	$[NiCl_3(py)]^-$	−1.18	−4.83	6.10	−2.44	−1.55	−0.38 (16)	−0.48 (20)
2c	$[NiI_3(py)]^-$	−1.11	−4.67	5.98	−2.42	−1.54	−0.41 (17)	−0.43 (29)
3a	$[PdH_3(NHC)]^-$	−1.63	−7.59	8.14	−2.45	−1.39	−0.37 (15)	−0.67 (27)
3b	$[PdCl_3(NHC)]^-$	−2.74	−10.19	11.59	−4.15	−2.98	−0.56 (13)	−0.57 (14)
3c	$[PdI_3(NHC)]^-$	−2.19	−9.23	10.75	−3.71	−2.72	−0.53 (14)	−0.43 (12)
4a	$[PdH_3(py)]^-$	−0.81	−3.95	4.70	−1.56	−0.80	−0.21 (13)	−0.50 (32)
4b	$[PdCl_3(py)]^-$	−1.19	−4.93	6.08	−2.34	−1.60	−0.34 (14)	−0.36 (15)
4c	$[PdI_3(py)]^-$	−0.77	−4.32	5.59	−2.04	−1.44	−0.35 (17)	−0.23 (11)
5a	$[PtH_3(NHC)]^-$	−1.73	−10.28	11.89	−3.32	−2.09	−0.43 (13)	−0.77 (23)
5b	$[PtCl_3(NHC)]^-$	−2.97	−12.89	15.03	−5.11	−3.79	−0.57 (11)	−0.72 (14)
5c	$[PtI_3(NHC)]^-$	−2.78	−12.14	14.33	−4.98	−3.77	−0.60 (12)	−1.58 (12)
6a	$[PtH_3(py)]^-$	−0.88	−5.36	6.68	−2.19	−1.33	−0.25 (11)	−0.55 (25)
6b	$[PtCl_3(py)]^-$	−1.40	−6.54	8.36	−3.22	−2.32	−0.38 (12)	−0.48 (15)
6c	$[PtI_3(py)]^-$	−1.04	−6.15	8.03	−2.92	−2.17	−0.40 (14)	−1.35 (13)

[a] Energies in eV.
[b] In parentheses is given the contribution of $\Delta E_{Orb}(b_1)$ and $\Delta E_{Orb}(b_2)$, respectively, to ΔE_{Orb}.

http://doc.rero.ch

been further probed by calculating the Mulliken and NPA orbital charge transfer from the filled π d_{yz} of the metal to the ligand. In complexes **3**, the Pd–NHC charge transfer amounts to 0.16e$^-$ for $[PdH_3(NHC)]^-$ **3a** and 0.10e$^-$ for $[PdCl_3(NHC)]^-$ and $[PdI_3(NHC)]^-$, **3b** and **3c**, respectively. In the corresponding pyridine complexes, charge transfer is virtually identical (0.18e$^-$ for **4a**, 0.09e$^-$ for **4b** and **4c**). Given the stronger σ bonding of NHC ligands, these values clearly suggest an enhanced π backbonding for the NHC ligand as compared with pyridine.

These results are supported by a quantitative analysis of the atomic charge variation upon ligand bonding to the $[MX_3]^-$ fragment. For this purpose, Hirshfeld atomic charges have been calculated for all complexes and the corresponding fragments, *viz*. $[MX_3]^-$ and L. Subsequent integration of the density difference between the fragments and the complex provided the charge variation at each atom upon bond formation. The differences for the most relevant nuclei are depicted in Fig. 6. The results unambiguously reveal that the charge transfer from NHC is larger than the one from pyridine. This supports the notion that the NHC ligand is a better donor than pyridine. Similar conclusions have been drawn from the preceding ETS analysis (vide supra). Furthermore, the electron density is increasing on the halide X_{trans}. This effect is more pronounced for the NHC complexes than for the pyridines and may reflect the higher *trans* influence of NHCs. Notably, the charge density at the metal center is considerably reduced when bound to hydrides. Such a pronounced π back bonding for hydride complexes $[MH_3L]^-$ corroborates the results from MO and energy decomposition analyses.

Furthermore, only little charge variation has been observed for the C–C backbone of the NHC ligand upon binding to the metal fragment. This indicates that the aromaticity is not particularly pronounced in these NHC ligands. For electronic considerations, the NHC ligand may therefore be split into an olefinic C=C part and an N–C–N 3-center-4-electron aminal system. Accordingly, little effect is expected from variation of the degree of saturation of the C–C bond. Such a conclusion corroborates earlier studies [29] and provides a rational for the activity of Grubbs' 2nd generation olefin metathesis catalysts, which are similar irrespective of whether the ruthenium-bound carbene is saturated or not [30].

3.4. Bond order

In addition to ETS, we have used bond order analysis as an approach to discuss the bonding based on the pioneering work of Mayer [17]. This method describes the interactions between pre-optimized fragment orbitals and is completely independent of the charges associated with these fragments. The only requested information for such analysis consists of the density and the overlap matrix, which are both available from DFT calculations.

Fig. 7 displays both bond order between the $[MX_3]^-$ and L fragments and between the metal and the coordinating nucleus of the ligand, *i.e*. C and N for NHC and pyridine, respectively. The π interaction has been extracted from the b_2 contribution relative to the total bond order. Except for the $[MH_3(py)]^-$ series, the relative π contribution does not depend strongly on whether the entire fragments or only the nuclei involved in the M–L bond are considered. According to both calculations, the relative b_2 contribution is predicted to be higher for complexes with pyridine than with carbene. This corroborates the preceding ETS analysis, in particular given the fact that the absolute π contributions are similar for pyridine and NHC bonding to these group 10 metals, while the σ term is much larger for NHC than for pyridine (vide supra). For the hydride complexes $[MH_3L]^-$, the fragment analysis produces generally a larger π contribution to the total bond order than the

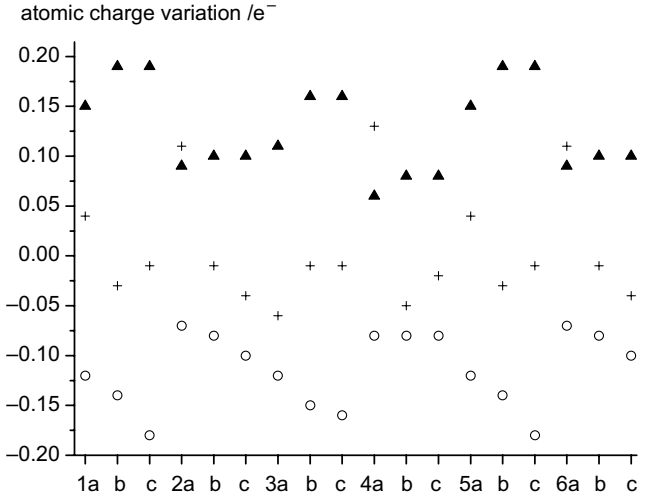

Fig. 6. Hirshfeld atomic charge variation on selected atoms upon combining the fragments L and $[MX_3]^-$, including the metal M (+), the ligand X_{trans} (○), and the coordinating atom N_{py} or C_{NHC} (▲).

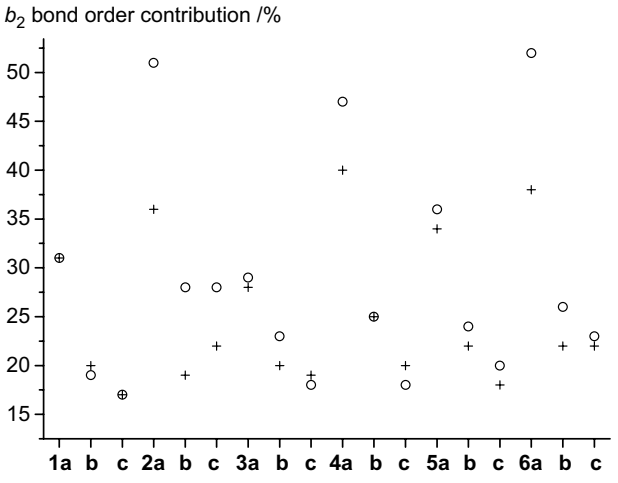

Fig. 7. Bond order decomposition analysis of $[MX_3L]^-$ complexes using $[MX_3]^-$–L fragment–fragment (○) or M–L atom–atom bond order decomposition (+).

atomic approach using only M and L. This is consistent with the conclusions drawn from MO diagram analysis.

4. Conclusion

We have used a combination of theoretical tools to compare the nature of the M–L bond between group 10 metals and NHC and py ligands in complexes of the type $[MX_3L]^-$. Molecular orbital (MO), extended transition state (ETS) methods, atomic charge variation, bond order decomposition, and charge transfer analyses consistently indicate that σ bonding of NHCs is considerably stronger than that of pyridines. The π acceptor interactions generally increase from $I \leqslant Cl < H$ as a consequence of the higher charge density on the metal in the MX_3^- fragment. The absolute π bonding is stronger for NHC than for pyridine. However, the relative contribution to the bond strength is calculated to be larger for pyridine due to the large σ term in the M–NHC bond. These results corroborate experimental findings that suggest strongly related donor ability of NHC and pyridine ligands in iron(II) complexes [7g], hence contributing to a better description of the bonding nature of NHC-type ligands.

Moreover, the fragment bond-order approach used to investigate the ambiguity of the charge assigned to each fragment extends the utility of frontier orbital and symmetry theory. The obtained results are in good agreement with MO, ETS and charge variation analysis.

http://doc.rero.ch

Acknowledgement

This work was supported by the Swiss National Science Foundation. M.A. is very grateful for an Alfred Werner Assistant Professorship.

Appendix A. Supplementary material

Supplementary data associated with this article can be found, in the online version, at doi:10.1016/j.jorganchem.2007.09.033.

References

[1] J.P. Collman, L.S. Hegedus, J.R. Norton, R.G. Finke, Principles and Applications of Organotransition Metal Chemistry, University Science Books, Mill Valley (CA), 1987.
[2] (a) D. Bourissou, O. Guerret, F.P. Gabbai, G. Bertrand, Chem. Rev. 100 (2000) 39;
(b) K.J. Cavell, D.S. McGuinness, Coord. Chem. Rev. 248 (2004) 671;
(c) S. Diez-Gonzalez, S.P. Nolan, Coord. Chem. Rev. 251 (2007) 874;
(d) S.P. Nolan (Ed.), N-Heterocyclic Carbenes in Synthesis, Wiley, Weinheim, 2006.
[3] (a) H.W. Wanzlick, H.J. Schönherr, Angew. Chem., Int. Ed. 7 (1968) 141;
(b) K. Öfele, J. Organomet. Chem. 12 (1968) P42;
(c) D.J. Cardin, B. Cetinkaya, E. Cetinkaya, M.F. Lappert, J. Chem. Soc., Dalton Trans. (1973) 514;
(d) P.J. Fraser, W.R. Roper, F.G.A. Stone, J. Chem. Soc., Dalton Trans. (1974) 760.
[4] A.J. Arduengo, R.L. Harlow, M. Kline, J. Am. Chem. Soc. 113 (1991) 361.
[5] T.M. Trnka, R.H. Grubbs, Acc. Chem. Res. 34 (2001) 18.
[6] (a) W.A. Herrmann, Angew. Chem., Int. Ed. 41 (2002) 1290;
(b) M. Lee, C. Hu, Organometallics 23 (2004) 976;
(c) N. Fröhlich, U. Pidun, M. Stahl, G. Frenking, Organometallics 16 (1997) 442;
(d) M.K. Samantaray, D. Roy, A. Patra, R. Stephen, M. Saikh, R.B. Sunoj, P. Ghost, J. Organomet. Chem. 691 (2006) 3797.
[7] (a) A.J. Arduengo, S.F. Gamper, J.C. Calabrese, F. Davidson, J. Am. Chem. Soc. 116 (1994) 4391;
(b) A.D.D. Tulloch, A.B. Danopoulos, S. Kleinhenz, M.E. Light, M.B. Hursthouse, G. Eastham, Organometallics 20 (2001) 2027;
(c) X. Hu, I. Castro-Rodriguez, K. Olsen, K. Meyer, Organometallics 23 (2004) 755;
(d) S. Saravankumar, A.I. Oprea, M.K. Kindermann, P.G. Jones, J. Heinicke, Chem. Eur. J. 12 (2006) 3143;
(e) W.A. Herrmann, J. Schütz, G.D. Frey, E. Herdtweck, Organometallics 25 (2006) 2437;
(f) J.C. Green, B.J. Herbert, Dalton Trans. (2005) 1214;
(g) L. Mercs, G. Labat, A. Neels, A. Ehlers, M. Albrecht, Organometallics 25 (2006) 5648.
[8] (a) D.S. McGuinness, N. Saendig, B.F. Yates, K.J. Cavell, J. Am. Chem. Soc. 123 (2001) 4029;
(b) D. Nemcsok, K. Wichmann, G. Frenking, Organometallics 23 (2004) 3640;
(c) H. Jacobsen, A. Correa, C. Costabile, L. Cavallo, J. Organomet. Chem 691 (2006) 4350;
(d) L. Gagliardi, C.J. Cramer, Inorg. Chem. 45 (2006) 9442.
[9] (a) A. Diefenbach, F.M. Bickelhaupt, G. Frenking, J. Am. Chem. Soc. 122 (2000) 6449;
(b) A.J. Bridgeman, C.J. Empson, Chem. Eur. J. 12 (2006) 2252;
(c) T. Leyssens, D. Peeters, A.G. Orpen, J.N. Harvey, Organometallics 26 (2007) 2637.
[10] ADF2006.01, SCM, Theoretical Chemistry, Vrije Universiteit Amsterdam, The Netherlands. <http://www.scm.com>.
[11] (a) C. Fonseca Guerra, J.G. Snijders, G. te Velde, E.J. Baerends, Theor. Chem. Acc. 99 (1998) 391;
(b) G. te Velde, F.M. Bickelhaupt, E.J. Baerends, C. Fonseca Guerra, S.J.A. van Gisbergen, J.G. Snijders, T. Ziegler, J. Comput. Chem. 22 (2001) 931.
[12] S.H. Vosko, L. Wilk, M. Nusair, Can. J. Phys. 58 (1980) 1200.
[13] (a) J.P. Perdew, Y. Wang, Phys. Rev. B 33 (1986) 8822;
(b) J.P. Perdew, J.A. Chevary, S.H. Vosko, K.A. Jackson, M.R. Pederson, D.J. Singh, C. Fiolhais, Phys. Rev. B 46 (1992) 6671.
[14] (a) E. van Lenthe, E.J. Baerends, J.G. Snijders, J. Chem. Phys. 99 (1993) 4597;
(b) E. van Lenthe, E.J. Baerends, J.G. Snijders, J. Chem. Phys. 101 (1994) 9783;
(c) E. van Lenthe, A. Ehlers, E.J. Baerends, J. Chem. Phys. 110 (1999) 8943.
[15] J.E. Lennard-Jones, Trans. Faraday Soc. 25 (1929) 668.
[16] F. Hirshfeld, Isr. J. Chem. 16 (1977) 226.
[17] (a) I. Mayer, Chem. Phys. Lett. 97 (1983) 270;
(b) A.J. Bridgeman, G. Cavigliasso, L.R. Ireland, J. Rothery, J. Chem. Soc., Dalton Trans. (2001) 2095;
(c) A.J. Bridgeman, G. Cavigliasso, J. Phys. Chem. A. 107 (2003) 4568.
[18] (a) K. Morokuma, Acc. Chem. Res. 10 (1977) 294;
(b) K. Morokuma, J. Chem. Phys. 55 (1971) 1236;
(c) K. Kitaura, K. Morokuma, Int. J. Quantum Chem. 10 (1976) 325.
[19] (a) T. Ziegler, A. Rauk, Theor. Chim. Acta 46 (1977) 1;
(b) T. Ziegler, A. Rauk, Inorg. Chem. 18 (1979) 1558;
(c) T. Ziegler, A. Rauk, Inorg. Chem. 18 (1979) 1755.
[20] A.E. Reed, R.B. Weinstock, F. Weinhold, J. Chem. Phys. 83 (1985) 735.

[21] (a) R.S. Mulliken, J. Chem. Phys. 23 (1955) 1833;
(b) R.S. Mulliken, J. Chem. Phys. 23 (1955) 2338.
[22] C. Fonseca Guerra, J.-W. Handgraaf, E.J. Baerends, F.M. Bickelhaupt, J. Comput. Chem. 25 (2004) 189.
[23] See the supplementary information for more details.
[24] E.D. Glendening, J.K. Badenhoop, A.E. Reed, J.E. Carpenter, J.A. Bohmann, C.M. Morales, F.Weinhold, NBO 5.0 Program, Madison, 2001.
[25] The Mathlab script used in this work is available on the internet, see: <www.chem.unifr.ch/cd>.
[26] (a) W.A. Herrmann, J. Schwarz, M.G. Gardiner, Organometallics 18 (1999) 4082;
(b) See also: R. Dinica, F. Marchetti, C. Pettinari, B.W. Skelton, A.H. White, Inorg. Chim. Acta 360 (2006) 2609.
[27] (a) A.A.D. Tulloch, S. Winston, A.A. Danopoulos, G. Eastham, M.B. Hursthouse, Dalton Trans. (2003) 699;
(b) See also: M. Konkol, C. Wagner, S. Schwieger, R. Lindner, D. Steinborn, Z. Anorg. Allg. Chem. 631 (2005) 1456.
[28] F.M. Bickelhaupt, E.J. Baerends, in: K.B. Lipkowitz, D.B. Boyd (Eds.), Reviews in Computational Chemistry, vol. 15, Wiley, New York, 2000.
[29] (a) C. Heinemann, T. Müller, Y. Apeloig, H. Schwarz, J. Am. Chem. Soc. 118 (1996) 2023;
(b) D.A. Dixon, A.J. Arduengo, J. Phys. Chem. A 110 (2006) 1968.
[30] (a) R.H. Grubbs, Angew. Chem., Int. Ed. 45 (2006) 3760;
(b) J. Huang, E.D. Stevens, S.P. Nolan, J.L. Petersen, J. Am. Chem. Soc. 121 (1999) 2674.

http://doc.rero.ch